



Published in final edited form as:

J Neuroimmunol. 2007 December ; 192(1-2): 40–48.

Dissociation of spinal microglia morphological activation and peripheral inflammation in inflammatory pain models

Ting Lin¹, Kai Li¹, Fei-Yu Zhang¹, Zhen-Kang Zhang¹, Alan R Light², and Kai-Yuan Fu¹

¹Center for TMD & Orofacial Pain, Peking University School & Hospital of Stomatology, Beijing 100081

²Dept. of Anesthesiology, University of Utah, Salt Lake City, Utah 84132-2304

Abstract

We compared the effects of peripheral Freund's Complete Adjuvant (CFA) and formalin injection on spinal microglia activation. Both qualitative and quantitative analyses showed signs of microglia activation on the ipsilateral side of the lumbar dorsal horn on day 3, day 7 and day 14 after formalin injection. However, significant microglia morphological alteration was not found in the CFA model. At the injection site in the paw, CFA injection induced considerably more inflammation than formalin injection. Although spinal microglia might be activated in inflammatory pain models, morphologically, spinal microglia activation was not closely correlated with peripheral inflammation.

Keywords

Microglia; Spinal cord; OX-42; Cyclooxygenase; Inflammation; Formalin

1. Introduction

Several laboratories have recently demonstrated that activated glia (microglia and astrocytes) in the spinal cord are key players in the induction and maintenance of pathological pain (Watkins et al., 2001; Tsuda et al., 2003; McMahon et al., 2005; Inoue, 2006). Spinal cord glia activation as detected with immunohistochemical markers for activated microglia and astrocytes has been demonstrated in almost all animal pain models, including neuropathic, traumatic injury, inflammatory, and bone cancer pain models (Gehrmann et al., 1991; Colburn et al., 1997; Molander C et al., 1997; Popovich et al., 1997; Coyle, 1998; Fu, et al., 1999; Sweitzer et al., 1999; Hashizume et al., 2000; Honore et al., 2000; Raghavendra et al., 2004). These exaggerated pain states are blocked by drugs that disrupt glial activation (Watkins et al., 1997; Hashizume et al., 2000b; Milligan et al., 2000; Sweitzer et al., 2001; Milligan et al., 2003; Raghavendra et al., 2003; Ledebor et al., 2005).

In neuropathic pain models, the temporal pattern of microglia activation as demonstrated with OX-42 immunohistochemistry (which labels complement receptor C3bi, also known as CD11b) is similar to the pattern of increased pain behavior. These previous time course experiments showed microglia activation in the superficial dorsal horn on the nerve injured

Corresponding author: Kai-Yuan Fu, DDS, PhD, Center for TMD & Orofacial Pain, Peking University School & Hospital of Stomatology, Beijing, 100081, PR China, Email: kqkyfu@bjmu.edu.cn, Tel: 86-10-62179977; Fax: 86-10-62173402. Corresponding author: Alan R. Light, Ph.D., Dept. of Anesthesiology, University of Utah, Salt Lake City, Utah 84132-2304, Email: Alan.Light@hsc.utah.edu.

Publisher's Disclaimer: This is a PDF file of an unedited manuscript that has been accepted for publication. As a service to our customers we are providing this early version of the manuscript. The manuscript will undergo copyediting, typesetting, and review of the resulting proof before it is published in its final citable form. Please note that during the production process errors may be discovered which could affect the content, and all legal disclaimers that apply to the journal pertain.

side as early as 24 h after peripheral nerve injury, which reached a maximum 7 to 14 days after injury (Colburn et al., 1997; Coyle, 1998; Hashizume et al., 2000a).

While the involvement of microglia in neuropathic pain is convincing, the involvement of microglia in inflammatory pain models is still questionable. Raghavendra et al. reported an increase of OX-42 immunostaining and other microglia activation marker mRNAs in the lumbar spinal cord following injection of Complete Freund's Adjuvant (CFA) into the rat hind paw, correlating with microglia activation and the enhancement of pain (Raghavendra et al., 2004). However, several other studies were unable to find the increase of OX-42 immunoreactivity over a similar time course with the same stimulus or with another inflammatory chemical irritant, mustard oil (Molander et al., 1997; Honore et al., 2000; Zhang et al., 2003; Clark et al., 2007). Spinal injection of the glial metabolic inactivator fluorocitrate (which can block astrocyte function, but the effects of which on microglia are unknown) attenuated ipsilateral hyperalgesia and bilateral spinal microglia activation after peripheral nerve injury (Clark et al., 2007). In contrast intrathecal fluorocitrate produced no attenuation of CFA-induced hyperalgesia (Clark et al., 2007). This failure to reverse the established CFA-induced hyperalgesia in conjunction with the observed minimal microglia activation suggests that the time course of microglia activation and its contribution to inflammatory pain is dependent on the inflammatory stimulus administered. The biological mechanisms behind these differences are unknown.

Subcutaneous formalin injection has an acute irritant effect and has long been used as a model of acute inflammatory pain. However, we have found that peripheral formalin injection also has longer-term tissue and nerve injury effects (Fu et al., 2001; Zhang et al., 2007). We previously reported robust microglia activation in the medial portion of the dorsal horn and in the gracile nucleus of the brainstem on the side ipsilateral to the formalin injection into the rat hind paw, starting on day 1-3 and peaking at day 7 post-injection (Fu et al., 1999). The time course of the microglia activation paralleled hyperalgesic responses to thermal and mechanical stimuli applied to the paw surface opposite the injected site (Fu et al., 2001).

In the present study, we compared spinal microglia activation and tissue inflammation of the injected hind paw following formalin and CFA injection respectively into the rat hind paw. This allowed comparison of a relatively "pure" inflammatory model (CFA injection) with a tissue damage/inflammation model (formalin injection). We found that, while CFA injection induced much more severe paw tissue inflammation, it did not cause substantial spinal microglia morphological changes. Tissue damage, inflammation or nerve injury may result in chronic neuropathic pain, and spinal microglia modulates the development and maintenance of chronic pain state. From our study, it is clear that spinal microglia activation as observed morphologically was not closely correlated with peripheral inflammation. Morphologically observable spinal microglia activation may be related to nerve injury which occurs in neuropathic and the formalin animal pain models, but which is less obvious in inflammatory pain models.

2. Materials and Methods

2.1. Animals and treatments

Experiments were performed on adult (200-225 g) male Sprague-Dawley rats. All rats were housed at a constant temperature of 22°C on a 12/12 hour light/dark cycle with food and water available ad libitum. Experimental rats in the formalin model group received subcutaneous injections of 100 µl 5% formalin (diluted in 0.9 % saline) into the plantar surface of the right hind paw. Rats in the CFA model group were injected subcutaneously into the right hind paw with 100µl CFA (Sigma, St. Louis, USA) suspended in an oil/saline (1:1) emulsion. The control group rats were injected with 100 µl 0.9% saline instead of formalin or CFA. The treatment

and care of all animals used in the study were approved by, and followed the guidelines of, the Peking University Medical Sciences Center Animal Welfare Committee.

2.2. Behavioral testing

Thermal and mechanical behavioral parameters of all groups were measured on day 0 (before injection), 6hrs, day 3, day 7 and day 14 after CFA (N=8), formalin (N=6), and saline (N=8) injection into rat plantar hind paw. Thermal hyperalgesia was assessed using a modified method of Hargreaves et al (1988). Briefly, the rats were habituated to a transparent plastic chamber on a glass plate preheated to a constant temperature. A mobile radiant heat source was located under the plate and focused on the plantar hind paw, and the paw withdrawal latencies were defined as the time for the rat to remove its hind paw from the glass. A cut-off time of 20s was used to avoid tissue damage to the hind paws.

To quantify mechanical sensitivity of the paw, rats were placed in clear plastic cages on an elevated mesh floor and allowed to acclimate for 30 min. Paw withdrawal thresholds (PWTs) to mechanical stimulus were determined using the up and down method by applying calibrated von Frey filaments (Stoelting Co., Wood Dale, IL) (Chaplan et al., 1994), or directly using electronic von Frey anesthesiometer (IITC Life Science, CA, USA) from underneath the cage through openings in the floor. Each trial was repeated 3 times at approximately 5 min intervals, and the mean value was used as the force to produce withdrawal responses.

2.3. Spinal OX-42 Immunohistochemistry

Animals (three to five rats at each time point) received subcutaneous injections of 100 μ l 5% formalin or CFA. Twelve rats served as controls (three at each time point) and were injected with saline into the right hind paw. Rats were anesthetized at 6hrs, 3 days, 7 days and 14 days following injection with an overdose of pentobarbital sodium and euthanized by transcardiac perfusion (250 ml body temperature 0.1M PBS pH 7.4 followed by 300 ml ice-cold 4% paraformaldehyde/4% sucrose in 0.1M PB pH 7.4). After perfusion, the lumbar spinal cord (L4-5) and the injected side of footpads were removed, postfixed in 4% paraformaldehyde fixative for 4 hours and then placed in a 30% sucrose solution (in 0.1 M PBS) overnight at 4 $^{\circ}$ C. Thirty micron thick spinal cord sections were cut transversely on a cryostat and processed for OX-42 immunohistochemical staining using the avidin-biotin technique (Elite Kit, Vector, Burlingame, CA), primary antibody was OX-42 (monoclonal mouse anti-rat CD11b, also called CR-3) (1:500, Serotec U.K.), as reported previously (Fu et al., 1999). In our experiments, replacement of primary antibody by mouse IgG2a, or PBS resulted in no staining.

Five no treatment rats were sacrificed and used for baseline staining for quantitative analysis. The sections from formalin injected rats and CFA injected rats along with saline injected controls were always processed together for comparison under the same conditions.

2.4. Evaluation of microglia morphological changes

Every third section was labeled with OX-42 and observed under low and high magnification to evaluate microglia morphological changes. We used the same semi-quantitative assessment of activation as previously described by Colburn et al (1997) and Wu et al (2004). These criteria are briefly described here.

- 1) **Baseline staining** (Fig 1A,1B), microglia cells are extensively ramified with fine processes that are evenly distributed throughout the dorsal horn (Fig2A).
- 2) **Mild increase** (Fig1C), microglia cells are ramified and evenly spaced with a slight increase in the number or intensity of cells (Fig2B), both medially and superficially in the dorsal horn.

- 3) **Moderate and localized** (Fig1D), microglia cells have shortened and clumpy processes (Fig2C) and more are found densely packed in the medial dorsal horn. Microglia activation spreads laterally and dorsoventrally, and leaves little or no space between cells.
- 4) **Maximal staining** (Fig1F,1H), a dark staining dot in the medial dorsal horn can be seen without a microscope. Under the microscope, microglia exhibit extremely hypertrophic (Fig2C) and only short, thick processes with extensive overlap. Microglia activation is spread into deep dorsal horn, extending to the central canal.

2.5. Quantitative analysis of microglia OX-42 immunoreactivity

Briefly, five successive sections from the lumbar spinal cord at the level of L4 ~ L5 were analyzed under light microscopy using a 4X objective with a computer-based image analysis system (JAVA Video Analysis Software). The medial half portion of the dorsal horn was outlined for quantitative analysis. Details of this method have been described previously (Fu et al., 1999). The area of interest was digitized via a video camera (Fig 3). The area within the field of interest covered by OX-42-IR profiles (red color area) relative to the total area of the measured field was automatically measured, and this value represented the relative proportion of the measured area that expressed OX-42 in the dorsal horn. Measurements were made on the ipsilateral sides from all animals. All data were expressed as fold increase compared to no-treatment control animals which were considered to be 1 fold.

2.6. Cyclooxygenase-1 and -2 (COX-1 and COX-2) immunohistochemistry and cell counting procedure

Peripheral tissues from the footpads (0.5cm × 0.5cm size) of the injected hind paw were cut into two halves through the injected point. Six-micrometer-thick sections were cut on a cryostat and thaw-mounted on pre-cleaned gelatin-coated glass slides, and kept at -80°C until used. After pretreatment in 0.3% H₂O₂ in methanol and 5% normal goat serum (NGS) or normal horse serum (NHS) in 0.01M PBS, sections were incubated in a polyclonal rabbit anti-murine COX-2 (1:200, Cayman, Ann Arbor, MI) diluted in 0.01M PBS containing 5% NGS or mouse monoclonal anti-ovine COX-1 antibody (1:400, Cayman, Ann Arbor, MI) diluted in 0.01M PBS containing 5% NHS. Subsequently, the sections were incubated in either biotinylated goat anti-rabbit or horse anti-mouse IgG (Vector) and further processed using Elite Vectastain ABC kit (Vector) according to the manufacturer instructions. Omission of primary antibody or replacement of primary antibody by PBS, or normal serum resulted in negative staining in all sections.

For COX-2 quantitation in the hind paw tissue, four sections were randomly selected from each rat. The images of immunostained sections were captured with a CCD camera, and labeled round inflammatory cells in a 20 optic field on each section were counted.

2.7. Statistical analysis

All data were reported as the mean ± SEM for each treatment-group of animals. ANOVA for repeated measurements followed by Bonferroni post-hoc tests were used for comparing paw withdrawal latency (threshold) in CFA and saline control group. Paired Students' *t*-test was performed to compare paw withdrawal latency and mechanical threshold in formalin test. For quantitative microglia activation and hind paw COX-2-positive cell counting, differences between groups (formalin and CFA group) and between time points were analyzed using two-way ANOVA followed by Tukey or Bonferroni post-hoc tests. The criterion for statistical significance was *P*<0.05.

3. Results

3.1. Time course of pain behavior induced by peripheral formalin and CFA injection

Peripheral CFA injection into the rat plantar hind paw caused significant behavioral hypersensitivity. The ipsilateral paw withdrawal thresholds to both thermal and mechanical stimuli were significantly reduced in the CFA- vs. saline-treated rats (Fig 4). The paw withdrawal thresholds were decreased at 6 hours after injection (the beginning of test) and lasted at least 2 weeks (the end of the experiment).

However, formalin injected rats did not respond to thermal and mechanical stimuli that were applied to the plantar surface of the rat hind paw (same surface injected with formalin) at the 6h and day 3 time points. Responses were detected at day 7 and day 14, but both thermal withdrawal latency and mechanical withdrawal threshold were significantly higher than the baseline (Table).

3.2. Peripheral formalin, not CFA treatment, induced spinal microglia morphological alteration

In saline and non-treatment control animals, OX-42 immunoreactivity (OX-42-IR) was homogeneously distributed throughout the spinal gray and white matter. Labeled resident microglia (ramified microglia) consisted of cells that appeared to be in a resting state; they had long finely branched processes that extended in all directions from the perinuclear cytoplasm. Three days after formalin administration into the plantar surface of hind paw, OX-42-IR was significantly increased in the medial portion of the L4-5 dorsal horn on the side ipsilateral to the injection (Fig 1D). These microglia cells appeared to be in an activated state (Fig2C). Although they still had ramified morphology, they were clearly hypertrophic and intensely stained compared to the resting microglia in saline control. The alteration was maximal on day 7 post-injection (Fig 1F, Fig 5). At this time, a dark stained dot could be seen without magnification in the ipsilateral, medial dorsal horn. With the microscope, microglia exhibited extremely hypertrophic and short, thick processes with dense overlap. Microglia activation spread into the deep dorsal horn, extending to the central canal.

However, we did not find marked increases in expression of OX-42 labeled microglia in the CFA-injected animals (Fig1A, 1E, 1G). We observed a mild increase in OX-42 immunoreactivity on the ipsilateral side of the spinal cord in only 2 of 5 animals on day 3 after CFA injection (Fig 1C, Fig 2B), and did not observe any increases at other time points.

We also compared spinal OX-42 immunoreactivity between formalin- and CFA-injected treatments by computer-aided quantitative analysis. Increases of OX-42-IR on the ipsilateral side of the lumbar dorsal horn following formalin injection were significantly higher than the CFA-injected group on day 3, day 7 and day 14, while no significant increase of OX-42 expression was found between the CFA- and saline- injected group (Fig 5).

3.3. CFA treatment induced much greater peripheral inflammation than formalin injection in the paw

Both formalin and CFA injection subcutaneously into the rat hind paw produced significant inflammation characterized by paw edema and redness. The inflammation occurred minutes after injection and was maintained for 1-2 weeks. CFA injection induced typical inflammatory reactions observed as large accumulations of neutrophils representative of acute inflammation (Fig 6B). Neutrophil increases were observed at 6hrs and day 3, and chronic inflammation characterized by the fibrosis and the infiltration of mononuclear cells was seen on day 14. Inflammatory cells were strongly stained with COX-2 (Fig 6E), but lightly labeled with COX-1 (data not shown). Originally observed with inflammatory cells, COX-2 was upregulated as an

immediate-early gene in response to inflammatory injury (Tomlinson et al., 1994; Katori et al., 1995). In the present study, COX-2 immunoreactivity was quantitatively regarded as an inflammatory marker and used for comparing CFA and formalin-injected groups (saline injected animals demonstrated no inflammatory cells with COX-2 positive at any time points).

However, formalin injections produced different histological changes, with many fewer inflammatory cells, but some macrophages, observed at 6hrs and day 3 (Fig 6C). At 2 weeks after formalin injection, we noted chronic inflammation similar to that seen with CFA injection. We quantitatively compared COX-2 immunoreactivity between formalin- and CFA-treated animals in the injected hind paw tissues. This comparison showed significantly more COX-2 positive inflammatory cells in CFA-treated than in formalin-treated groups at 6hrs, day 3 and day 14 post-injections (Fig 7). In the CFA group, the maximal COX-2 expression was found at 6hrs after injection (Fig6E, Fig7), which was significantly more than that at day 3 ($p < 0.05$) and day 14 ($p < 0.001$). However, there were no significant differences in the formalin group at any of the three time points (Fig7).

Animals receiving saline injections did not develop signs of inflammation (Fig 6A), with only a few fibroblasts in saline injected tissue observed to be very lightly stained with COX-2 (Fig 6D, 6G).

4. Discussion

4.1. CFA injection produces more severe peripheral inflammation, but does not cause significant spinal microglia morphological changes

Microglia respond to peripheral nerve injury by progressing through a series of stereotypical morphological changes. Upon an unknown stimulus (possibly ATP), microglia move from a resting (ramified) form to an activated form and may progress ultimately to a reactive (phagocytic) form. The transformation of spinal microglia detected by immunohistochemistry for OX-42, which labels complement receptor type 3 (CR3) on microglia, has been most completely characterized in nerve injury animal pain models, which have consistently shown morphological changes with microglia increasing in number and increasing in density of staining with OX-42 immunohistochemistry (Gehrmann et al., 1991; Colburn et al., 1997; Coyle, 1998; Hashizume et al., 2000a; Honore et al., 2000). Similarly, in other reports, damage to nerves (facial nerve axotomy and nerve electrical stimulation) also showed a similar pattern of microglia activation as observed with OX-42 labeling (Graeber et al., 1988; Molander et al., 1997).

Peripheral formalin injection has long been used as a model of inflammation (Dubuisson and Dennis, 1977; Tjolsen et al., 1992; Porro and Cavazzuti, 1993). We had previously also found that robust spinal microglia activation was caused by formalin injection (Fu et al., 1999). This contrasts with the experiments reported here that demonstrate that the rat inflammatory pain model produced by intraplantar injection of CFA causes only minor morphological changes in spinal microglia. Further, no significant quantitative increase in spinal OX-42 labeling was observed at any time point. We found that CFA induced much more severe inflammatory reactions as indicated by the accumulation of inflammatory cells and COX-2 positive staining in the vicinity of the injections, compared with formalin injection. In spite of the much greater inflammatory response in the paw caused by CFA, microglia morphological changes and OX-42 immunostaining in the ipsilateral lumbar spinal cord was considerably less than with formalin injection. The comparison between CFA and formalin pain model suggests that inflammation at the injection site may not be responsible for the activated microglia morphological changes.

4.2. Microglia are likely reacting to peripheral injury at times before morphological alteration

Microglia activation with morphological changes was evident as early as 2-3 days after peripheral tissue injury (Graeber et al., 1988; Gehrmann et al., 1991; Colburn et al., 1997; Molander et al., 1997; Coyle, 1998; Fu et al., 1999; Hashizume et al., 2000a; Honore et al., 2000). Recently, other indicators of microglia and astrocyte activation such as ITGAM, TLR4, CD14, MHC class II, IL-1beta and other cytokines, were used to verify the glial activation (Raghavendra et al., 2004; Tanga et al., 2004). These markers showed increases at earlier time-points than OX-42 labeling has shown in these and other studies cited above. Another group used carrageenan injection into the hind paw to evoke inflammation. They observed an increase in MAP kinase (p38) in spinal microglia within 60 minutes after injection (Hua et al., 2005). Intrathecal administration of minocycline (a functional microglia inhibitor) blocked carrageenan induced hyperalgesia, and also attenuated the increased phosphorylation of p38 in microglia. These reports indicate that microglia are capable of reacting to peripheral inflammatory inputs at times well before morphological alterations can be observed with OX-42. Microglia could be activated rapidly without any changes in obvious morphological or staining characteristics which have previously been used to characterize the resting-to-activated transition (Hua et al., 2005). It appears that even in the resting state, microglia are functionally active (Hua et al., 2005; Nimmerjahn et al., 2005). Other reports indicate that peripheral formalin injection also can increase phosphorylation of p38 in microglia within 5 minutes after injection, and pretreatment with p38 MAPK inhibitors could suppress paw flinching behaviors and spinal neuronal fos expression (Svensson et al., 2003). So spinal microglia activation is likely to have two states: one with and one without cell morphological alteration.

4.3. Nerve injury causes profound morphological activation of microglia, while inflammation causes little spinal microglia morphological alteration

Although animals showed spontaneous pain behaviors within 90 min following formalin injection, the formalin injected surface of the rat hind paw did not respond to thermal and mechanical stimuli at 6h and 3 day time points. The loss of responsiveness of the injected site caused by formalin was also reported in an electrophysiological study, and this loss of sensory input caused by formalin injection was interpreted to be the result of injury of the peripheral nerve terminals (Chen and Koyama, 1998). We have previously reported similar hypoalgesia in the formalin damaged region using the hot-plate test and mechanical tests. However, the un-injected side (plantar side when injected into dorsal surface, dorsal side when injected into plantar surface) showed hyperalgesia (Fu et al., 2001). Formalin, although a potent nociceptive activator, also causes irreparable damage to the site of injection due to protein cross-linking (Winter and McCarron, 2005). We looked at PGP9.5, CGRP and Substance P labeling in the vicinity of formalin injection, and found this procedure eliminated the intraepidermal nerve fiber staining (data not shown). These findings suggest that 5% formalin injection damages the local nociceptive receptors at the injection site, and results in the loss of responses to thermal and mechanical stimuli.

Our present interpretation of spinal microglia activation by formalin injection is that the activation is induced by the nerve injury, not the tissue inflammation, both of which are produced by formalin injection. Other inflammatory pain models do induce microglia activation as observed with OX-42 immunohistochemistry. For example, perisciatic administration of zymosan (a model of sciatic inflammatory neuropathy, SIN) significantly increased OX-42 expression with microglia morphological changes in the ipsilateral dorsal horn (Ledeboer et al., 2005). However, subcutaneous injection of zymosan into the rat hind paw did not induce robust microglia morphological activation (Sweitzer et al., 1999). It was suggested in the former report that zymosan induced peripheral nerve injury, not tissue inflammation, caused spinal microglia morphological activation. Similarly, peripheral nerve

exposure to the HIV-1 envelope protein gp120 could lead to chronic painful peripheral neuropathy, and also produced more robust microglia activation in the absence of infectivity (Herzberg and Sagen, 2001). Taken together, these observations suggest that nerve injury is required for substantial morphological activation of spinal cord microglia.

In the present report, we show that CFA can induce enhanced pain lasting at least 2 weeks, without causing marked spinal microglia morphological changes. It appears that spinal microglia morphological alteration is not necessary for long-term enhanced pain caused by inflammation of the paw. Interestingly, a recent report by Ledeboer et al (2006) demonstrated that an animal model of deep pain (intramuscular acidic saline injection), that causes long-term allodynia, does not cause either morphological microglia activation or other cytokine markers of microglia activation. In addition, the allodynia produced by this model is not affected by agents that block glial function. Also a very recent report demonstrated that intrathecal fluorocitrate administration (which can block microglia activation, possibly through an indirect mechanism) did not reverse intraplantar CFA-induced hyperalgesia (Clark et al., 2007). Thus, it is possible that when morphologically observable activation of microglia and the pain enhancement that is mediated by this activation is observed in inflammatory pain models, the microglia activation is caused not by inflammation, per se, but by nerve injury induced by the stimulus used to activate inflammation.

Acknowledgements

The research was supported by program for New Century Excellent Talents in University (NCET) and Project 30371544 by National Natural Science Foundation of China and P01-NS039429 from the National Institute of Health, USA.

References

- Chaplan SR, Bach FW, Pogrel JW, Chung JM, Yaksh TL. Quantitative assessment of tactile allodynia in the rat paw. *J Neurosci Methods* 1994;53(1):55–63. [PubMed: 7990513]
- Chen J, Koyama N. Differential activation of spinal dorsal horn units by subcutaneous formalin injection in the rat: an electrophysiological study. *Exp Brain Res* 1998;118(1):14–18. [PubMed: 9547073]
- Clark AK, Gentry C, Bradbury EJ, McMahon SB, Malcangio M. Role of spinal microglia in rat models of peripheral nerve injury and inflammation. *Eur J Pain* 2007;11(2):223–230. [PubMed: 16545974]
- Colburn RW, DeLeo JA, Rickman AJ, Yeager MP, Kwon P, Hickey WF. Dissociation of microglial activation and neuropathic pain behaviors following peripheral nerve injury in the rat. *J Neuroimmunol* 1997;79(2):163–175. [PubMed: 9394789]
- Coyle DE. Partial peripheral nerve injury leads to activation of astroglia and microglia which parallels the development of allodynic behavior. *Glia* 1998;23(1):75–83. [PubMed: 9562186]
- Dubuisson D, Dennis SG. The formalin test: a quantitative study of the analgesic effects of morphine, meperidine, and brain stem stimulation in rats and cats. *Pain* 1977;4(2):161–174. [PubMed: 564014]
- Fu KY, Light AR, Matsushima GK, Maixner W. Microglial reactions after subcutaneous formalin injection into the rat hind paw. *Brain Res* 1999;825(12):59–67. [PubMed: 10216173]
- Fu KY, Light AR, Maixner W. Long-lasting inflammation and long-term hyperalgesia after subcutaneous formalin injection into the rat hindpaw. *J Pain* 2001;2(1):2–11. [PubMed: 14622781]
- Gehrmann J, Monaco S, Kreutzberg GW. Spinal cord microglial cells and DRG satellite cells rapidly respond to transection of the rat sciatic nerve. *Restorative Neurology and Neuroscience* 1991;2:181–198.
- Graeber MB, Streit WJ, Kreutzberg GW. Axotomy of the rat facial nerve leads to increased CR3 complement receptor expression by activated microglial cells. *J Neurosci Res* 1988;21(1):18–24. [PubMed: 3216409]
- Hargreaves K, Dubner R, Brown F, Flores C, Joris J. A new and sensitive method for measuring thermal nociception in cutaneous hyperalgesia. *Pain* 1988;32(1):77–88. [PubMed: 3340425]
- Hashizume H, DeLeo JA, Colburn RW, Weinstein JN. Spinal glial activation and cytokine expression after lumbar root injury in the rat. *Spine* 2000a;25(10):1206–1217. [PubMed: 10806496]

- Hashizume H, Rutkowski MD, Weinstein JN, DeLeo JA. Central administration of methotrexate reduces mechanical allodynia in an animal model of radiculopathy/sciatica. *Pain* 2000b;87(2):159–169. [PubMed: 10924809]
- Herzberg U, Sagen J. Peripheral nerve exposure to HIV viral envelope protein gp120 induces neuropathic pain and spinal gliosis. *J Neuroimmunol* 2001;116(1):29–39. [PubMed: 11311327]
- Honore P, Rogers SD, Schwei MJ, Salak-Johnson JL, Luger NM, Sabino MC, Clohisy DR, Mantyh PW. Murine models of inflammatory, neuropathic and cancer pain each generates a unique set of neurochemical changes in the spinal cord and sensory neurons. *Neuroscience* 2000;98(3):585–598. [PubMed: 10869852]
- Hua XY, Svensson CI, Matsui T, Fitzsimmons B, Yaksh TL, Webb M. Intrathecal minocycline attenuates peripheral inflammation-induced hyperalgesia by inhibiting p38 MAPK in spinal microglia. *Eur J Neurosci* 2005;22(10):2431–2440. [PubMed: 16307586]
- Inoue K. The function of microglia through purinergic receptors: Neuropathic pain and cytokine release. *Pharmac Therap* 2006;109(12):210–226.
- Katori M, Harada Y, Hatanaka K, Majima M, Kawamura M, Ohno T, Aizawa A, Yamamoto S. Induction of prostaglandin H synthase-2 in rat carrageenin-induced pleurisy and effect of a selective COX-2 inhibitor. *Adv Prostaglandin Thromboxane Leukot Res* 1995;23:345–347. [PubMed: 7732867]
- Ledeboer A, Sloane EM, Milligan ED, Frank MG, Mahony JH, Maier SF, Watkins LR. Minocycline attenuates mechanical allodynia and proinflammatory cytokine expression in rat models of pain facilitation. *Pain* 2005;115(12):71–83. [PubMed: 15836971]
- Ledeboer A, Mahoney JH, Milligan ED, Martin D, Maier SF, Watkins LR. Spinal cord glia and interleukin-1 do not appear to mediate persistent allodynia induced by intramuscular acidic saline in rats. *J Pain* 2006;7(10):757–767. [PubMed: 17018336]
- McMahon SB, Cafferty WB, Marchand F. Immune and glial cell factors as pain mediators and modulators. *Exp Neurol* 2005;192(2):444–462. [PubMed: 15755561]
- Milligan ED, Mehmert KK, Hinde JL, Harvey LO, Martin D, Tracey KJ, Maier SF, Watkins LR. Thermal hyperalgesia and mechanical allodynia produced by intrathecal administration of the human immunodeficiency virus-1 (HIV-1) envelope glycoprotein, gp120. *Brain Res* 2000;861(1):105–116. [PubMed: 10751570]
- Milligan ED, Twining C, Chacur M, Biedenkapp J, O'Connor K, Poole S, Tracey K, Martin D, Maier SF, Watkins LR. Spinal glia and proinflammatory cytokines mediate mirror-image neuropathic pain in rats. *J Neurosci* 2003;23(3):1026–1040. [PubMed: 12574433]
- Molander C, Hongpaisan J, Svensson M, Aldskogius H. Glial cell reactions in the spinal cord after sensory nerve stimulation are associated with axonal injury. *Brain Res* 1997;747(1):122–129. [PubMed: 9042535]
- Nimmerjahn A, Kirchhoff F, Helmchen F. Resting microglial cells are highly dynamic surveillants of brain parenchyma in vivo. *Science* 2005;308(5726):1314–1318. [PubMed: 15831717]
- Popovich PG, Wei P, Stokes BT. Cellular inflammatory response after spinal cord injury in Sprague-Dawley and Lewis rats. *J Comp Neurol* 1997;377(3):443–464. [PubMed: 8989657]
- Porro CA, Cavazzuti M. Spatial and temporal aspects of spinal cord and brainstem activation in the formalin pain model. *Prog Neurobiol* 1993;41(5):565–607. [PubMed: 8284437]
- Raghavendra V, Tanga F, DeLeo JA. Inhibition of microglial activation attenuates the development but not existing hypersensitivity in a rat model of neuropathy. *J Pharmacol Exp Ther* 2003;306(2):624–630. [PubMed: 12734393]
- Raghavendra V, Tanga FY, DeLeo JA. Complete Freund's adjuvant-induced peripheral inflammation evokes glial activation and proinflammatory cytokine expression in the CNS. *Eur J Neurosci* 2004;20(2):467–473. [PubMed: 15233755]
- Svensson CI, Marsala M, Westerlund A, Calcutt NA, Campana WM, Freshwater JD, Catalano R, Feng Y, Protter AA, Scott B, Yaksh TL. Activation of p38 mitogen-activated protein kinase in spinal microglia is a critical link in inflammation-induced spinal pain processing. *J Neurochem* 2003;86(6):1534–1544. [PubMed: 12950462]
- Sweitzer SM, Colburn RW, Rutkowski M, DeLeo JA. Acute peripheral inflammation induces moderate glial activation and spinal IL-1beta expression that correlates with pain behavior in the rat. *Brain Res* 1999;829(12):209–221. [PubMed: 10350552]

- Sweitzer SM, Schubert P, DeLeo JA. Propentofylline, a glial modulating agent, exhibits antiallodynic properties in a rat model of neuropathic pain. *J Pharmacol Exp Ther* 2001;297(3):1210–1217. [PubMed: 11356948]
- Tanga FY, Raghavendra V, DeLeo JA. Quantitative real-time RT-PCR assessment of spinal microglial and astrocytic activation markers in a rat model of neuropathic pain. *Neurochem Int* 2004;45(2):397–407. [PubMed: 15145554]
- Tjolsen A, Berge OG, Hunskaar S, Rosland JH, Hole K. The formalin test: an evaluation of the method. *Pain* 1992;51(1):5–17. [PubMed: 1454405]
- Tomlinson A, Appleton I, Moore AR, Gilroy DW, Willis D, Mitchell JA, Willoughby DA. Cyclooxygenase and nitric oxide synthase isoforms in rat carrageenin-induced pleurisy. *Br J Pharmacol* 1994;113(3):693–698. [PubMed: 7532080]
- Tsuda M, Shigemoto-Mogami Y, Koizumi S, Mizokoshi A, Kohsaka S, Salter MW, Inoue K. P2X4 receptors induced in spinal microglia gate tactile allodynia after nerve injury. *Nature* 2003;424(6950):778–783. [PubMed: 12917686]
- Watkins LR, Martin D, Ulrich P, Tracey KJ, Maier SF. Evidence for the involvement of spinal cord glia in subcutaneous formalin induced hyperalgesia in the rat. *Pain* 1997;71(3):225–235. [PubMed: 9231865]
- Watkins LR, Milligan ED, Maier SF. Spinal cord glia: new players in pain. *Pain* 2001;93(3):201–205. [PubMed: 11514078]
- Winter MK, McCarron KE. G-protein activation by neurokinin-1 receptors is dynamically regulated during persistent nociception. *J Pharmacol Exp Ther* 2005;315(1):214–221. [PubMed: 15985614]
- Wu Y, Willcockson HH, Maixner W, Light AR. Suramin inhibits spinal cord microglia activation and long-term hyperalgesia induced by formalin injection. *J Pain* 2004;5(1):48–55. [PubMed: 14975378]
- Zhang J, Hoffert C, Vu HK, Groblewski T, Ahmad S, O'Donnell D. Induction of CB2 receptor expression in the rat spinal cord of neuropathic but not inflammatory chronic pain models. *Eur J Neurosci* 2003;17(12):2750–2754. [PubMed: 12823482]
- Zhang FY, Wan Y, Zhang ZK, Light AR, Fu KY. Peripheral formalin injection induces long-lasting increases in cyclooxygenase 1 expression by microglia in the spinal cord. *J Pain* 2007;8(2):110–117. [PubMed: 16949875]

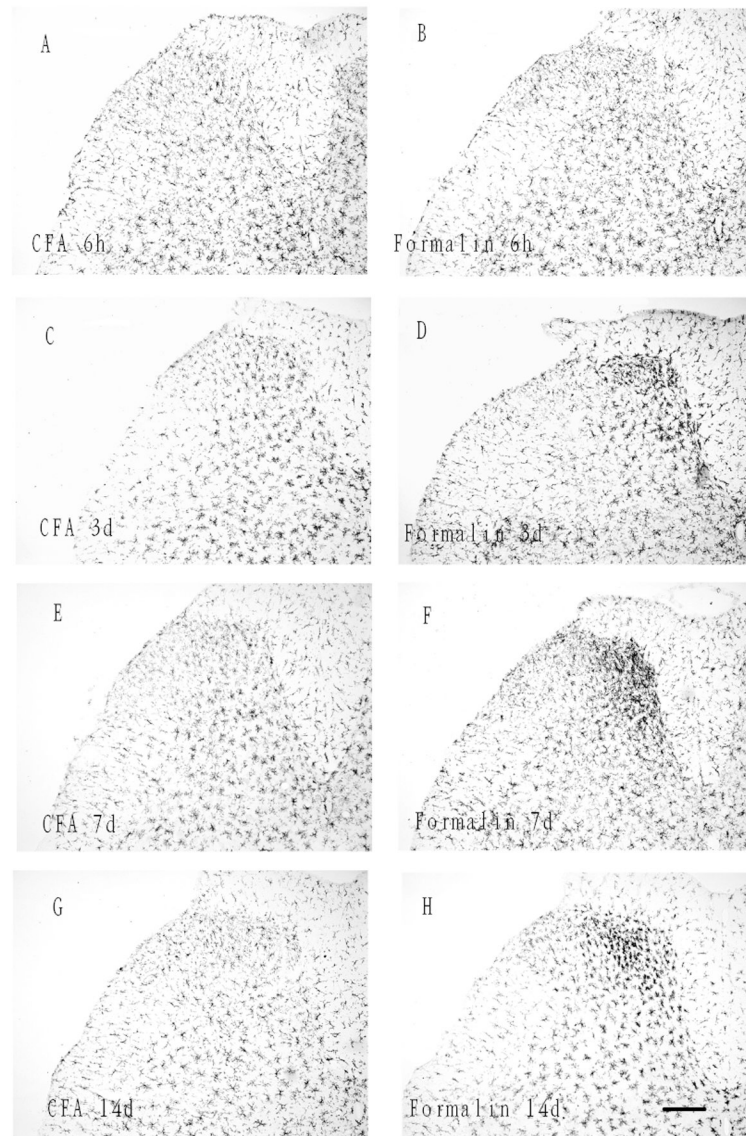


Fig 1. OX-42 immunoreactivity in the ipsilateral side of lumbar spinal cord following CFA (A,C,E,G) and formalin (B,D,F,H) injection. No increase was found following CFA injection at 6 hrs (A), day 7 (E) and day 14 (G); slight increase of staining intensity in the medial portion of superficial dorsal horn at day 3 (C). Significant increases of both the number of microglia and staining intensity in the medial portion of dorsal horn were observed following formalin injection at day 3 (D), day 7 (F) and day 14 (H). However, no significant increases were observed at 6hrs (B). Scale bar 120 μ m.

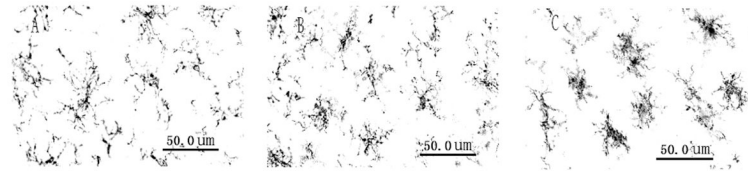


Fig 2. Higher magnification images of microglia showing morphological changes. A: Ramified microglia with fine processes from 3 day saline injected control animal; B: A slight increase of OX-42 staining without obviously morphological change from 3 day CFA injected animal; C: Ramified morphology but clearly hypertrophic with much shorter and thickened processes from 3 day formalin injected animal appearing to be in an activated state.

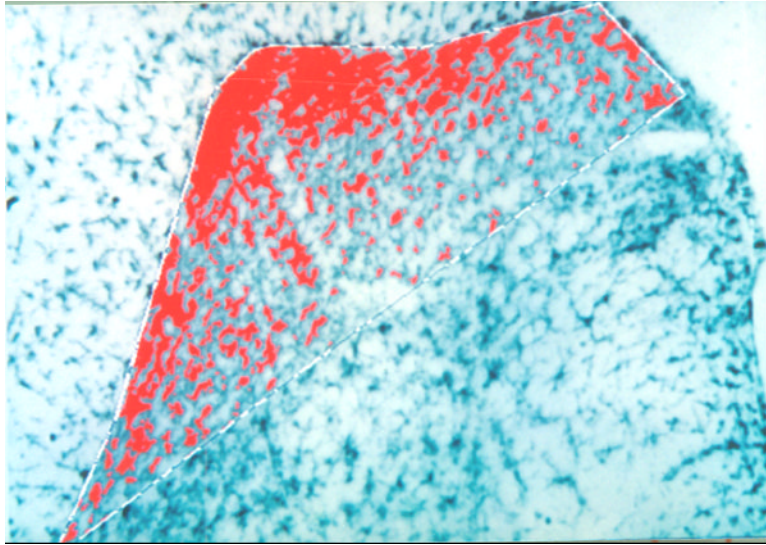


Fig 3. OX-42 labeled, computerized image of the regions selected for quantitative analysis. The red area within the interested region represents the area counted as immunolabeled.

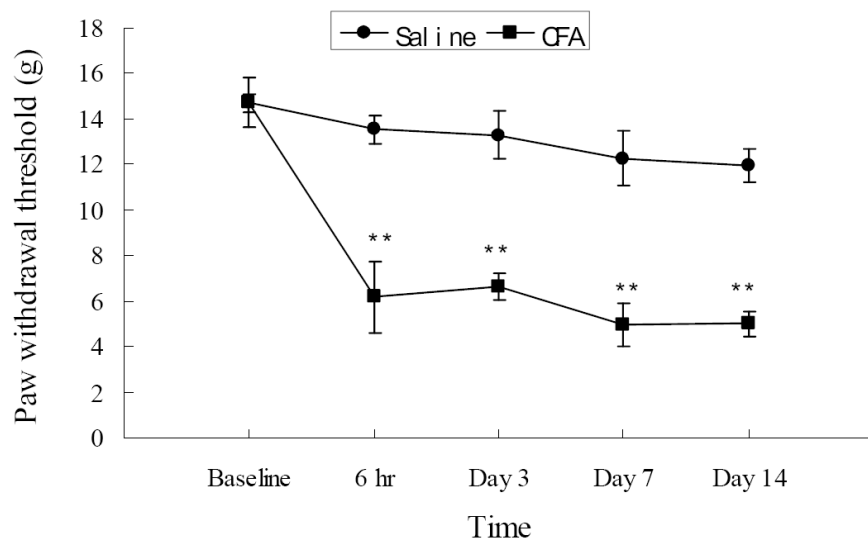
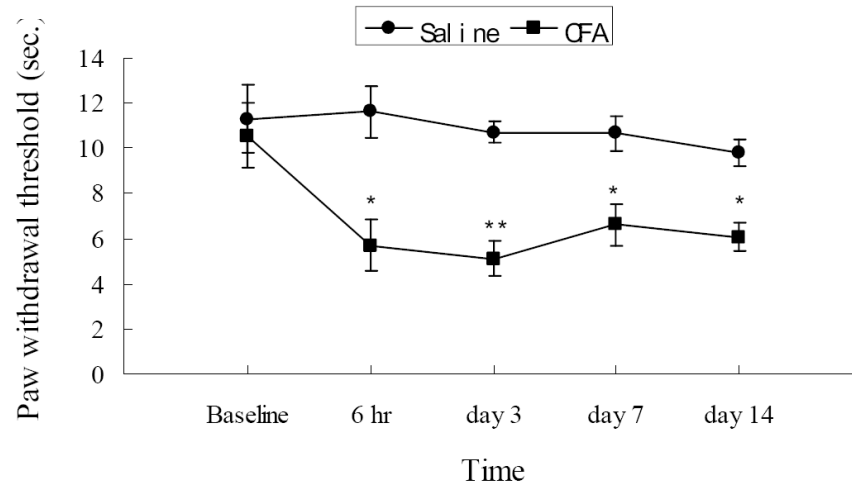


Fig 4. Time courses of CFA-induced thermal and mechanical hyperalgesia. Top: Paw withdrawal latency in seconds measured on day 0, 6hrs, day3, day7 and day 14 after intraplantar injection of CFA or saline. Bottom: Paw withdrawal threshold as determined with monofilament bending in grams at the same time points as in the figure above. * $P < 0.05$, ** $P < 0.01$ compared to baseline (N=8).

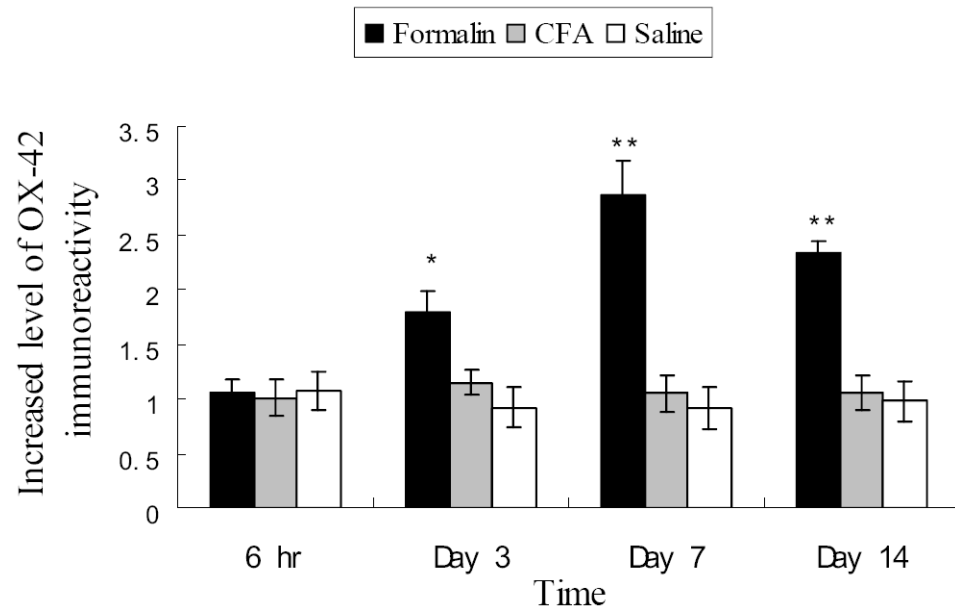


Fig 5. Time course of the ipsilateral spinal dorsal horn OX-42-IR following CFA and formalin injection, showing the relationship between the survival time and the intensity of CFA- or formalin-induced microglia activation. * $P < 0.05$, ** $P < 0.01$ compared to the saline control group.

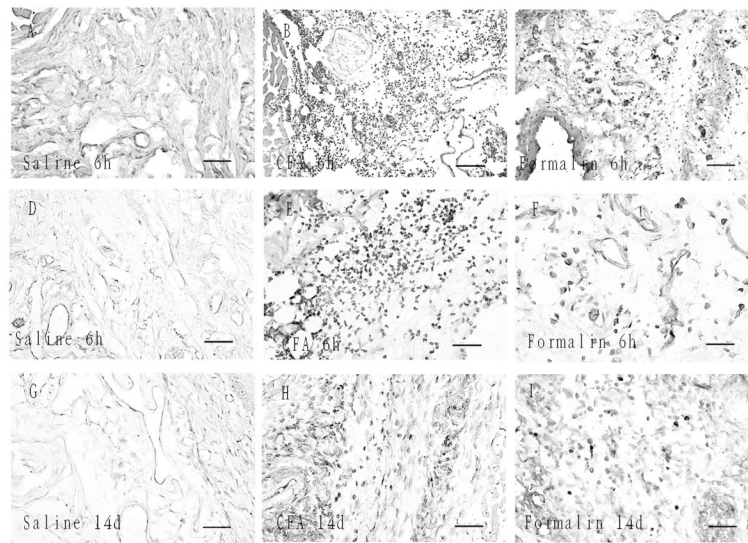


Fig 6. Photomicrographs of H&E staining (A,B,C) and COX-2 immunohistochemical staining (D-I) from saline, CFA and formalin injected hind paw. Large accumulations of neutrophils were observed following CFA injection at 6 hrs (B). Few inflammatory cells but some macrophages were found at 6hrs following formalin injection (C), compared to saline injected control (A). Scale bar 100 μ m. The inflammatory cells were strongly stained with COX-2 at 6hrs and shown significantly more COX-2 positive inflammatory cells in CFA-treated (E) than in formalin-treated (F) group. D is saline control. The COX-2 immunoreactivity significantly decreased at day 14 both in CFA (H) and formalin (I) groups. G is saline control. Scale bar 50 μ m.

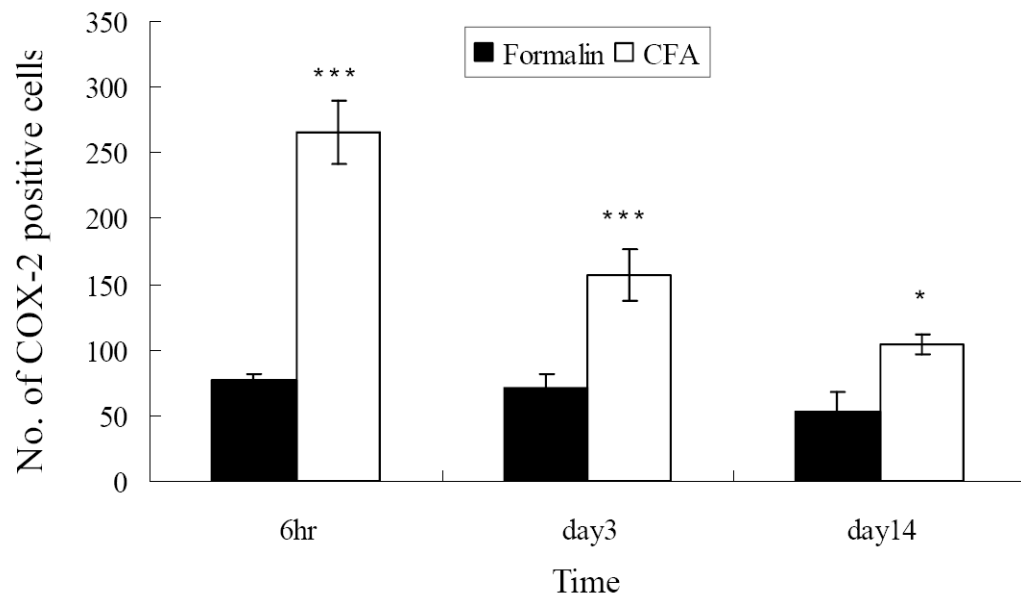


Fig 7. Quantitative comparison of COX-2 immunoreactive cell numbers in the injected hind paw tissues between CFA- and formalin-treated animals. * $P < 0.05$, *** $P < 0.001$ compared to formalin-treated group.

Time course of thermal and mechanical stimulated pain responses on the plantar surface following formalin was injected into the plantar hind paw

Table

	Baseline	6 hours	3days	7 days	14 days
Paw withdrawal latency(s)	13.02±0.71	NR	NR	18.31±1.07*	16.33±2.07*
Paw withdrawal threshold(g)	25.6±0.8	NR	NR	46.2±3.5**	42.5±5.2**

Paw withdrawal thresholds were determined using digital electronic von Frey anesthesiometer (IITC Life Science, CA, USA). Each value is Mean ± S.E.M., NR, no response

* P<0.05

** P<0.01 vs corresponding baseline.